Pharmacokinetics and pharmacodynamics of oral oxycodone in healthy human subjects: Role of circulating active metabolites

Background: **In vitro experiments suggest that circulating metabolites of oxycodone are opioid receptor agonists. Clinical and animal studies to date have failed to demonstrate a significant contribution of the *O*-demethylated metabolite oxymorphone toward the clinical effects of the parent drug, but the role of other putative circulating active metabolites in oxycodone pharmacodynamics remains to be examined.**

Methods: **Pharmacokinetics and pharmacodynamics of oxycodone were investigated in healthy human volunteers; measurements included the time course of plasma concentrations and urinary excretion of metabolites derived from *N*-demethylation, *O*-demethylation, and 6-keto-reduction, along with the time course of miosis and subjective opioid side effects. The contribution of circulating metabolites to oxycodone pharmacodynamics was analyzed by pharmacokinetic-pharmacodynamic modeling. The human study was complemented by in vitro measurements of opioid receptor binding and activation studies, as well as in vivo studies of the brain distribution of oxycodone and its metabolites in rats.**

Results: **Urinary metabolites derived from cytochrome P450 (CYP) 3A–mediated *N*-demethylation of oxycodone (noroxycodone, noroxymorphone, and α- and β-noroxycodol) accounted for 45% ± 21% of the dose, whereas CYP2D6-mediated *O*-demethylation (oxymorphone and α- and β-oxymorphol) and 6-keto-reduction (α- and β-oxycodol) accounted for 11% ± 6% and 8% ± 6% of the dose, respectively. Noroxycodone and noroxymorphone were the major metabolites in circulation with elimination half-lives longer than that of oxycodone, but their uptake into the rat brain was significantly lower compared with that of the parent drug. Pharmacokinetic-pharmacodynamic modeling indicated that the time course of pupil constriction is fully explained by the plasma concentration of the parent drug, oxycodone, alone. The metabolites do not contribute to the central effects, either because of their low potency or low abundance in circulation or as a result of their poor uptake into the brain.**

Conclusions: **CYP3A-mediated *N*-demethylation is the principal metabolic pathway of oxycodone in humans. The central opioid effects of oxycodone are governed by the parent drug, with a negligible contribution from its circulating oxidative and reductive metabolites. (Clin Pharmacol Ther 2006;79:461-79.)**

Bojan Lalovic, PhD, Evan Kharasch, MD, PhD, Christine Hoffer, BS, Linda Risler, BS, Lee-Yuan Liu-Chen, PhD, and Danny D. Shen, PhD *Seattle, Wash, and Philadelphia, Pa*

Oxycodone is a widely prescribed oral opioid. Since the introduction of controlled-release oxycodone in 1995, annual prescriptions of oxycodone in the United States have increased by several-fold.[1,2] The analgesic potency of intravenous oxycodone is nearly the same as that of intravenous morphine (equianalgesic dose ratio of 1.3); hence, it is classified as a step 3 strong opioid in the World

From the Departments of Pharmaceutics, Pharmacy, Medicinal Chemistry, and Anesthesiology, University of Washington, and Division of Clinical Research, Fred Hutchinson Cancer Research Center, Seattle, and Department of Pharmacology, Temple University, Philadelphia.

Supported in part by the following grants from the National Institutes of Health: R01-AT00864 (D.D.S.), K24-DA00417 (E.K.), R01-DA11263 (L.-Y.L.-C.), P30-DA13429 (L.-Y.L.-C.), and M01-RR00037 to the University of Washington General Clinical Research Center.

Received for publication Aug 16, 2005; accepted Jan 3, 2006.

Reprint requests: Danny D. Shen, PhD, Department of Pharmacy, University of Washington, Box 357630, Seattle, WA 98195.
E-mail: *ds@u.washington.edu*

0009-9236/$32.00

doi:10.1016/j.clpt.2006.01.009

Health Organization pain ladder for management of moderate to severe cancer pain.[1,3,4]

There is a widespread notion that active metabolites contribute significantly to the clinical pharmacologic characteristics of oxycodone. An earlier study by Kalso et al[5] suggested the presence of pharmacologically active metabolites in circulation after the oral administration of oxycodone. Displacement of tritium-labeled dihydromorphine binding to rat brain homogenates by plasma extracts from subjects administered oxycodone was greater than that expected on the basis of the concentration of intact oxycodone in plasma as measured by gas chromatography. For a while, it was thought that oxymorphone, which is formed from 3-*O*-demethylation of oxycodone by cytochrome P450 (CYP) 2D6, represented the principal activating pathway, a situation analogous to the bioconversion of codeine to morphine. Morphine derived from *O*-demethylation of codeine has been shown to account for most, if not all, of the analgesic activity of codeine.[6,7] Oxymorphone is a remarkably potent μ-opioid ligand, with 2 to 5 times higher μ-opioid receptor affinity and in vivo analgesic potency than morphine.[8–11] However, recent data showed that inhibition of oxymorphone formation by the CYP2D-selective inhibitor quinine or quinidine did not decrease the antinociceptive effect of oxycodone in rats.[12] Moreover, pretreatment with quinidine did not attenuate the opioid side effects of oral oxycodone in human volunteers, despite a 50-fold reduction in oxymorphone area under the plasma concentration–time curve (AUC).[13,14] The question thus arises as to whether the prevailing assumption of active metabolites governing the pharmacodynamics of oxycodone is correct or whether the putative active metabolite or metabolites arise from non-CYP2D6 pathways of oxycodone metabolism.

An earlier in vitro metabolic study from our laboratory showed that *O*-demethylation accounts for merely 13% of oxycodone oxidative metabolism in human liver microsomes.[15] Oxidation of oxycodone occurs largely via *N*-demethylation by CYP3A4/5 to noroxycodone, which is the most abundant metabolite in circulation after the administration of oxycodone in human subjects.[13,14] Noroxycodone exhibits weak antinociceptive potency in rats; however, it undergoes further oxidative metabolism to noroxymorphone, which is known to be a more potent displacer of [^{3}H]–(D-Ala^2, *N*-Me-Phe^4, Gly-ol^5)-enkephalin (DAMGO) from μ-opioid receptor in rat brain homogenates as compared with oxycodone.[16,17] We have also shown that oxycodone undergoes reductive metabolism to α- and β-oxycodol in vitro (Fig 1).[15] Likewise, reduction of noroxycodone to α- and β-noroxycodol and reduction of oxymorphone to α- and β-oxymorphol are feasible. There is no available information on the opioid receptor binding characteristics of these reduced metabolites. Some or all of these primary and secondary metabolites of oxycodone may contribute to the analgesia and side effects of oxycodone, provided that they have sufficiently high affinity and efficacy at the opioid receptor(s), are present in high concentrations in circulation, and are accessible to the central nervous system.

The overall objective of our study was to investigate whether the pharmacodynamics of oxycodone in humans is entirely attributed to the pharmacokinetics of oxycodone or involves the additional contribution of the aforementioned metabolites arising from non-CYP2D6 pathways. Initially, a series of in vitro experiments were conducted to compare the binding affinity (inhibition constant [K_i]) and receptor potency and efficacy (ie, guanosine-5′-*O*-[γ-thio(triphosphate)] [GTPγS] binding) of oxycodone and its metabolites by use of recombinant opioid receptors. We then characterized the plasma concentration–time profile of the oxidative (ie, noroxycodone, oxymorphone, and noroxymorphone) and reductive (ie, α- and β-oxycodol, α- and β-noroxycodol, and α- and β-oxymorphol) metabolites after a single oral dose of oxycodone in healthy human subjects. The time course of pupil constriction and the subjective side effects of oxycodone were measured simultaneously. Pharmacokinetic-pharmacodynamic (PK-PD) analysis was performed by use of both the in vivo data from healthy subjects and the in vitro receptor data in an attempt to seek evidence that would support or refute the hypothesis that circulating metabolites contribute to the pharmacodynamics of oxycodone. In addition, we obtained supplemental data on the uptake of oxycodone and its metabolites into the brain after intraperitoneal injections of oxycodone in rats.

METHODS

Chemicals and reagents. Morphine, oxycodone, noroxycodone, and oxymorphone were obtained from Cerilliant (Austin, Tex). Epimers of oxycodol, noroxycodol, and oxymorphol were synthesized by respective chemical reduction of oxycodone, noroxycodone, and oxymorphone as previously described.[18] DAMGO, cyclic (D-Pen^2, D-Pen^5)-enkephalin, and guanosine 5′-diphosphate (GDP) were obtained from Sigma-Aldrich (St Louis, Mo). U50,488 was obtained from Research Biochemicals International (Natick, Mass), and GTPγS was purchased from Roche Biochemicals (Palo Alto, Calif). [^{3}H]-Diprenorphine (50 Ci/mmol) and sulfur 35–labeled GTPγS (1250 Ci/mmol) were supplied by PerkinElmer Life and Analytical Sciences (Boston,

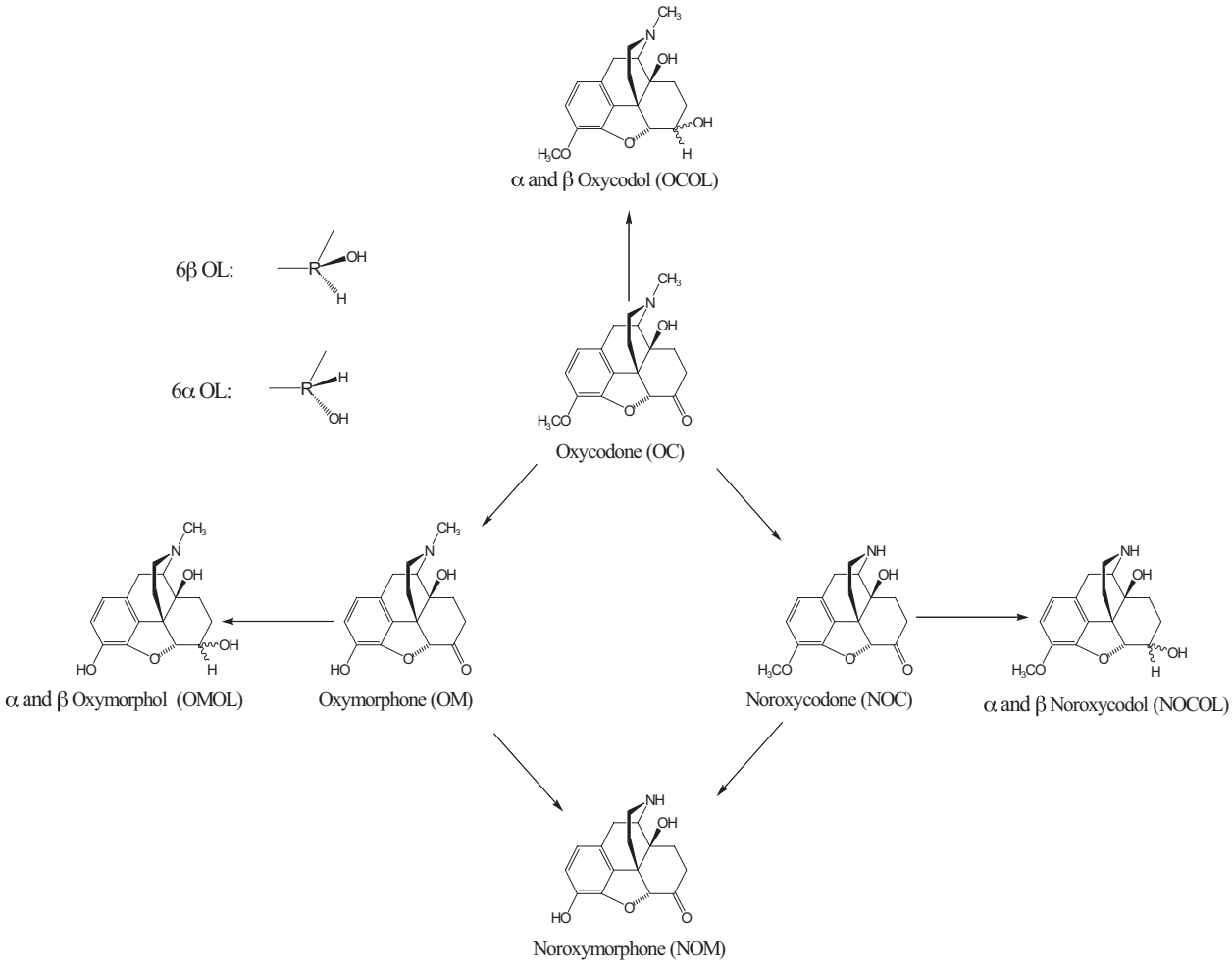

Fig 1. Metabolic scheme of oxycodone depicting oxidative and reductive pathways of parent drug and its metabolites.

Mass). Polypropylene 500-μL 96-well plates were purchased from Fisher Scientific (Pittsburgh, Pa). Ninety-six–well GF/B-UniFilterplates from PerkinElmer Life and Analytical Sciences were used in both receptor affinity and activation assays. Stably expressed human μ-opioid receptor (hMOR1) in Chinese hamster ovary (CHO) cells was purchased from PerkinElmer Life and Analytical Sciences.

Radioligand displacement studies with recombinant opioid receptors. Cell membranes were prepared from CHO-K1 cells that stably express the mouse δ-opioid receptor and the human κ-opioid receptor according to previously described procedures.[19–22] The interaction of oxycodone and its metabolites with each of the recombinant opioid receptor subtypes was assessed by their displacement of the high-affinity radioligand [^{3}H]-diprenorphine. The test ligand at concentrations ranging from 0.1 pmol/L to 1 μmol/L was incubated in duplicate with 0.4-nmol/L [^{3}H]-diprenorphine and 30 μg/mL CHO-K1 cell membrane protein in 400 μL of 50-mmol/L Tris(hydroxymethyl)aminomethane (Tris)–hydrochloric acid buffer (pH 7.4) for 1 hour at room temperature. Nonspecific binding was assessed in the presence of 10-μmol/L naloxone. Incubation was terminated by rapid filtration onto GF/B-UniFilterplates that were presoaked with 50 μL of 50-mmol/L Tris-HCl buffer (pH 7.4) by use of a Packard 96-well sample harvester (PerkinElmer Life and Analytical Sciences). The filter plates were then washed twice with 400 μL of 50-mmol/L Tris-HCl buffer (pH 7.4) and dried at 50°C for 1 hour. Forty microliters of Microscint 40 (PerkinElmer Life and Analytical Sciences) was then added to each well, and sample radioactivity was determined with a TopCount scintillation counter

(PerkinElmer Life and Analytical Sciences). Data represented as percent radioligand displaced against ligand concentration were fitted to the Hill equation by nonlinear regression by use of the SAAM II program (SAAM Institute, Seattle, Wash). K_i for the competitive displacement of [^{3}H]-diprenorphine by oxycodone and its metabolites, as well as control ligands, was calculated by use of the Cheng-Prusoff equation. The dissociation constant (K_d) of diprenorphine for the human μ-opioid receptor was provided by the supplier of hMOR1 or was available from literature for the κ- and δ-opioid receptors.[20]

^{35}S-GTPγS binding assay. Agonist-stimulated [^{35}S]-GTPγS binding to G_α proteins was determined by a modified procedure described by Huang et al[20] and Gillen et al.[23] Membranes from CHO cells transfected with human μ-opioid receptor were thawed rapidly, diluted in 50 mmol/L *N*-[2-hydroxyethyl]piperazine-*N*′-[2-ethanesulfonic acid] (HEPES) buffer (pH 7.4), and resuspended by homogenization. Membranes at a final protein concentration of 30 μg/mL were added to 50-mmol/L HEPES buffer (pH 7.4) containing 5-mmol/L magnesium chloride, 100-mmol/L sodium chloride, 1-mmol/L ethylenediaminetetraacetic acid, 15-μmol/L GDP, 0.4-nmol/L [^{35}S]-GTPγS, and ligand at concentrations varying from 100 pmol/L to 100 μmol/L to a final volume of 400 μL. After 1 hour of incubation at 37°C, bound [^{35}S]-GTPγS was separated by filtration onto the GF/B-UniFilterplates and counted for radioactivity, as described previously. Each incubation was performed in duplicate. Data represent the mean from at least 2 separate experiments. The ligand concentration at 50% of maximum receptor activation (EC_{50}) and maximum activation expressed as percent above basal [^{35}S]-GTPγS binding (E_{max}) of each agonist were estimated by fitting the binding data to the classical E_{max} model.[24]

Oxycodone PK-PD study. The University of Washington Institutional Review Board (Seattle, Wash) approved the human subject protocol. Each subject provided written informed consent. We enrolled 16 healthy white subjects (8 men and 8 women; age range, 21-30 years; mean weight, 73 ± 12 kg) in the study. Subjects were excluded if they were taking any prescription (including oral contraceptives) or over-the-counter medications known to alter CYP3A activity. Antidepressants, which have been shown to cause changes in pupil response, were also excluded.[25–27] Subjects were instructed to avoid grapefruit or grapefruit juice for at least 3 days before each study day and throughout the 48 hours after oxycodone administration. They were also asked to abstain from caffeine-containing beverages and alcohol for 24 hours before and throughout the 48-hour study period. They were instructed to fast for at least 8 hours before the start of the study.

The study was divided into 2 phases. During the first phase, 4 subjects (2 men and 2 women) were enrolled in a pilot dose-finding study. Each subject received 3 escalating doses of oxycodone (10, 15, and 20 mg) separated by at least 3 to 7 days between doses to allow for complete washout of oxycodone and its metabolites. The pilot study was intended to establish an optimal dose that allows a robust definition of the time course of oxycodone pharmacodynamics while avoiding the ceiling in pupil response and ensuring tolerable side effects. The main study was conducted in 12 subjects (6 men and 6 women) with a single 15-mg dose of oxycodone. All subjects were admitted into the University of Washington General Clinical Research Center for a 24-hour period and requested to return at 48 hours to turn in their 24- to 48-hour urine collection. At the beginning of each study day, an indwelling catheter was inserted into an arm vein for repetitive blood sampling. Subjects were monitored for signs of respiratory depression with a pulse oximeter for at least 4 hours after oxycodone administration. Venous blood samples (10 mL each) were obtained before and at 10, 30, 45, 60, 75, 90, 120, 180, 240, 360, 480, and 720 minutes after the administration of oral oxycodone. Plasma was separated from blood and stored at −20°C, pending analysis. Subjects were fed a light breakfast at 3 to 4 hours and had access to fluids and food thereafter. Cumulative urine samples were collected for the periods from 0 to 12 hours, 12 to 24 hours, and 24 to 48 hours.

Dark-adapted pupil diameter was measured before oxycodone administration and 5 minutes before each blood drawing by use of a Pupilscan Model 2 infrared pupillometer (Fairville Medical Optics, Newark, NJ) as described previously.[28] Constriction in pupil diameter in response to oxycodone was calculated by subtracting pupil diameter at various times from the baseline pupil diameter, which was defined by the mean of predose and 24-hour pupil diameters. The area under the effect curve (AUEC) was calculated by linear interpolation of the time course of pupil constriction. Subjective side effects of oxycodone were also recorded 5 minutes after each blood drawing by use of 10-cm visual analog scales (VASs) for alertness, nausea, pruritus, and general mood. On the alertness VAS, 10 indicated "wide awake" and 0 indicated "can't keep my eyes open." On the nausea VAS and pruritus VAS, 0 indicated "no nausea/itch at all" and 10 indicated "as much as possible." On the mood VAS, 10 indicated "the best I have

ever felt" and 0 indicated "the worst I have ever felt."[29,30]

Drug metabolite analysis. Plasma and urine samples were analyzed for concentrations of oxycodone and its metabolites (oxymorphone, noroxycodone, noroxymorphone, α- and β-oxycodol, α- and β-oxymorphol, and α- and β-noroxycodol) by use of a liquid chromatography–mass spectrometry (LC-MS) method adapted from our previously published method for oxycodone metabolites in human liver microsomes.[15]

For plasma analysis, 20 ng of deuterated internal standard (oxycodone-d_3) was added to 0.1 to 1 mL of samples in 3-mL screw-top polypropylene tubes, followed by 1.5 mL of 100-mmol/L borate buffer (pH 8.9). Each tube was capped, mixed in a vortex blender, and subjected to solid-phase extraction. Varian CERTIFY solid-phase extraction columns (C8/C18 mixed resin; Varian, Palo Alto, Calif) were preconditioned by passing 2 mL of methanol, followed by 2 mL of deionized water, through each column. Samples were loaded onto the extraction columns under reduced pressure (5-10 mm Hg). The loaded sample was washed with 4 mL of deionized water, followed by 1 mL of 0.1-mol/L acetic acid (pH 4) and 2 mL of methanol. Air was pulled through the columns at 20 mm Hg for 3 to 5 minutes. Analytes were eluted into 13 × 100–mm glass tubes by use of a 3-mL mixture of methylene chloride, isopropanol, and aqueous ammonium hydroxide (80:20:2 by volume). The organic solvent was evaporated under dry nitrogen at 60°C. Extracts were reconstituted with 100 μL mobile phase (mixture of 10-mmol/L acetate buffer and acetonitrile [85:15 by volume]), of which 2 to 5 μL was injected onto the LC-MS system.

To determine the total excretion of oxycodone and its metabolites, urine samples were subjected to enzymatic hydrolysis by use of β-glucuronidase and sulfatase. Aliquots of urine (0.05-0.1 mL) were diluted (1:2 [vol/vol]) with 50-μmol/L acetate buffer (pH 5.5). Twenty-five microliters of Type H-2 crude extract from *Helix pomatia* (Sigma-Aldrich) containing 2500 U β-glucuronidase and 500 U sulfatase was added to each sample. Samples were incubated for 24 hours at 60°C in 3-mL capped polypropylene plastic tubes. The incubation conditions have been shown to yield near-complete hydrolysis of morphine-3-glucuronide and morphine-6-glucuronide.[31] Samples were then spun, and the supernatants were prepared for LC-MS analysis in an identical manner to the plasma samples. To determine concentrations of unconjugated or free oxycodone and its metabolites, untreated urine samples (0.25 mL) were extracted in parallel and processed in the same manner. The conjugate fraction was estimated by subtracting the amount assayed in hydrolyzed samples from the amount assayed in unhydrolyzed samples.

Chromatographic separation of the analytes was achieved on a 5-μm, 2.1 × 150–mm Zorbax SSB C18 column (Agilent Technologies, Palo Alto, Calif). Gradient elution was programmed over a period of 20 minutes, followed by an 8-minute, postrun column re-equilibration period. The mobile phase consisted of a binary mixture of 10-mmol/L potassium acetate at pH 4 and acetonitrile, with the initial composition set at 95%:5% (vol/vol) of acetate/acetonitrile and held constant for 6 minutes at a flow rate of 0.225 mL/min. The flow rate was then increased during the next minute to 0.3 mL/min, and the acetonitrile content was then increased to 10% by 15 minutes, increased to 13.5% by 17 minutes, and then held constant until 20 minutes.

The mass spectrometer was operated in the atmospheric pressure ionization electrospray mode with positive polarity. Selective ion monitoring was set for ion channels corresponding to the molecular $[M+H^+]$ ions of the analytes as follows (with retention times in parentheses): oxycodone, mass-to-charge ratio (*m*/*z*) 316, and oxycodone-d_3, *m*/*z* 319 (18 minutes); oxymorphone, *m*/*z* 302 (6 minutes); noroxycodone, *m*/*z* 302 (16 minutes); noroxymorphone, *m*/*z* 288 (4 minutes); α- and β-oxymorphol, *m*/*z* 304 (3 and 3.5 minutes, respectively); α- and β-noroxycodol, *m*/*z* 304 (14 and 14.5 minutes, respectively); and α- and β-oxycodol, *m*/*z* 318 (15 and 15.5 minutes, respectively).

Quality control samples at multiple levels were included in each assay run. Interday coefficients of variation for replicate analysis of quality control samples was consistently less than 10%.

Pharmacokinetic analysis. The apparent clearance (CL/F) and volume of distribution (V_z/F) of oral oxycodone, along with the terminal elimination rate constant (λ_z) and corresponding half-life ($t_{½,z}$), maximum concentration (C_{max}), time to maximum concentration (t_{max}), and AUC extrapolated to infinity ($AUC_{0-\infty}$) of oxycodone and its metabolites, were estimated from their plasma concentration–time data by use of noncompartmental methods (WinNonlin 4.01 software; Pharsight, Mountain View, Calif). The metabolite–to–parent drug AUC ratios (AUC_m/AUC_p) were calculated to afford a comparison of the relative abundance of each metabolite in circulation. Oxycodone partial clearances via *N*-demethylation, *O*-demethylation, and 6-keto-reduction were calculated by multiplying oxycodone clearance by the fraction of dose recovered in the 48-hour urine collection as metabolites resulting from each primary metabolic pathway.

PK-PD modeling. A plot of the percent decrease in pupil diameter versus oxycodone plasma concentration over time demonstrated counterclockwise hysteresis, an observation consistent with either an equilibration delay between plasma and effect sites or a contribution of active metabolite(s) to the pupil response. To differentiate between these 2 possibilities, we compared the fit of 2 PK-PD models with the data: One model featured the joint action of the parent drug and its metabolites, and the alternate model featured the parent drug as the sole contributor to the miotic effect of oxycodone over time. To assess which of the metabolites most likely contributes to the pharmacodynamics of oxycodone, a simulation of μ-opioid receptor activation over time was performed for each of the circulating metabolites of oxycodone on the basis of its plasma concentration–time course and EC_{50} and E_{max} derived from the GTPγS binding assay. The simulation suggested that, of all of the metabolites in circulation, noroxymorphone has the highest likelihood of contributing to the miotic effect of oxycodone because of its abundance in circulation and potency in μ-receptor activation. As a result, only noroxymorphone was recognized as the contributory metabolite in the joint parent drug–metabolite PK-PD model.

PK-PD analysis was performed by use of the general-purpose compartmental modeling software SAAM II (SAAM Institute, Seattle, Wash).[32] Initial compartmental analysis of data from both the pilot and main studies indicated that 19 of 24 plasma oxycodone concentration–time profiles were adequately described by a 1-compartment model featuring first-order oral absorption with a variable lag time, whereas the other 5 profiles were better described by a 2-compartment model featuring first-order oral absorption. To avoid the complexity of identifying different compartmental model mixtures for the parent drug and its metabolite across subjects, forcing functions for the plasma concentrations of oxycodone and noroxymorphone over time were generated within SAAM II and used to drive the pharmacodynamic model.[33]

PK-PD models with or without an equilibration delay between plasma concentration and effect were evaluated. For the model without an equilibration delay, plasma concentration drives the effect. The equilibration-delay model features an effect compartment with a first-order rate constant (ke0) for the elimination of drug from the effect site.[34,35] Effect is then driven by the putative effect-site concentration. Equation 1 shows the effect-concentration relationship for the parent drug PK-PD model, and equation 2 shows the relationship for the joint parent drug–metabolite PK-PD model that describes the combined action of 2 agonists at a single receptor[24,36]:

$$E = E_0 \times \left(1 - \frac{Ce,\ oc^{\gamma}}{EC_{50,\,oc}{}^{\gamma} + Ce,\ oc^{\gamma}}\right) \quad (1)$$

$$E = E_o \times \left[1 - \left(\frac{\left(\frac{Ce,\ oc}{EC_{50,\,oc}}\right)^{\gamma} + \left(\frac{Ce,\ nom}{EC_{50,\,nom}}\right)^{\delta}}{1 + \left(\frac{Ce,\ oc}{EC_{50,\,oc}}\right)^{\gamma} + \left(\frac{Ce,\ nom}{EC_{50,\,nom}}\right)^{\delta}}\right)\right] \quad (2)$$

where Ce is the plasma or effect-site concentration, oc is oxycodone, EC_{50} is the concentration resulting in pupil constriction to 50% of the maximum, E_o is the baseline pupil diameter with the implicit assumption that E_{max} equals E_o (ie, there is complete constriction of the pupil at very high effect-site concentration), and nom is noroxymorphone. The parameters γ and δ are the Hill coefficients representing the steepness of the sigmoidal concentration-effect relationship.

For the parent drug PK-PD model with an equilibration delay, only a single ke0 estimate for oxycodone is needed. Initial estimates of the oxycodone equilibration rate constant for the effect site (ke0) were obtained by analyzing the hysteresis plot of plasma oxycodone concentration–effect–time data by use of the KE0 program.[37] This program collapses the hysteresis loop (ie, minimizes the area inscribed by the hysteresis loop by minimizing the distance between 2 equieffective concentration levels) by a nonparametric method developed by Unadkat et al.[38]

For the joint parent drug–noroxymorphone PK-PD model that features delayed equilibration, separate ke0 estimates for oxycodone and noroxymorphone were required. A naive plot of the pupil response against the noroxymorphone concentration showed an apparent counterclockwise hysteresis (albeit a less prominent loop than that observed with plasma oxycodone concentration data alone), which suggested the possibility of a distinct equilibration delay in effect with noroxymorphone. This apparent hysteresis was analyzed by the KE0 program utility yielding an initial estimate for the noroxymorphone ke0 parameter.

Brain distribution study in rats. The previously described PK-PD modeling is based entirely on plasma drug metabolite concentration data from human subjects. To further elucidate the contribution of metabolites to the pharmacodynamics of oxycodone in the central nervous system, the extent to which oxycodone and its metabolites are taken up into the brain was investigated in male Wistar rats (310-330 g) after intragastric administration of a 10-mg/kg dose of oxy-

Table I. Competitive displacement (K_i) of [^{3}H]-diprenorphine from its binding to membranes prepared from cultured cells stably expressing μ-, κ-, and δ-opioid receptor subtypes by oxycodone and its metabolites, along with opioid receptor subtype–specific ligands (DAMGO and morphine for μ-opioid receptor, U50,488 for κ-opioid receptor, and DPDPE for δ-opioid receptor)

	[^{3}H]-Diprenorphine displacement (K_i) (nmol/L)			*[^{35}S]-GTPγS binding to hMOR1*	
Ligand	*hMOR1*	*hKOR1*	*mDOR1*	*EC_{50} (nmol/L)*	*E_{max} (%)*
Oxycodone	16.0 ± 2.9	>1000	>1000	343 ± 7.9	234
α-Oxycodol	187 ± 36	>1000	>1000	6790 ± 180	246
β-Oxycodol	33.7 ± 5.9	>1000	>1000	1900 ± 46	242
Noroxycodone	57.1 ± 10	>1000	>1000	1930 ± 55	219
α-Noroxycodol	—	—	—	29,900 ± 1300	185
β-Noroxycodol	—	—	—	12,800 ± 890	149
Oxymorphone	0.36 ± 0.01	148 ± 17	118 ± 20	42.8 ± 0.8	261
α-Oxymorphol	—	—	—	221 ± 4.7	244
β-Oxymorphol	—	—	—	125 ± 3.3	213
Noroxymorphone	5.69 ± 1.1	87 ± 13	162 ± 29	167 ± 3.6	239
Morphine	3.19 ± 0.43	—	—	94.2 ± 1.9	252
DAMGO	0.21 ± 0.03	—	—	96.6 ± 1.4	315
U50,488	—	0.78 ± 0.31	—	—	—
DPDPE	—	—	2.0 ± 0.8	—	—

G-protein/opioid receptor complex activation by oxycodone and its metabolites, DAMGO, and morphine was characterized by sulfur 35–labeled GTPγS binding to cell membranes expressing the human μ-opioid receptor. Data from 2 independent experiments performed in duplicate were fitted to the E_{max} equation to yield estimates of EC_{50} and E_{max}. Dashes indicate that no data were available. Estimates of the SD of E_{max} (2 experiments performed in duplicate) were consistently lower than 1% for all determinations and are not reported for each ligand.

K_i, Inhibition constant; DAMGO, (D-Ala^2, *N*-Me-Phe^4, Gly-ol^5)-enkephalin; GTPγS, guanosine-5′-*O*-(γ-thio[triphosphate]); DPDPE, cyclic (D-Pen^2, D-Pen^5)-enkephalin; hMOR1, human μ-opioid receptor; hKOR1, human κ-opioid receptor; mDOR1, mouse δ-opioid receptor; EC_{50}, concentration at 50% of maximum receptor activation; E_{max}, maximum activation.

codone (approximately 3.0 mg in 1-mL volume). This dose is at the high end of the established intraperitoneal antinociceptive dose range in the rat (1-10 mg/kg).[12,39,40] At 60 minutes after dosing, which was previously observed to be the time of peak antinociceptive effect, the rats were anesthetized by intraperitoneal ketamine/xylazine. Blood samples were obtained by cardiac puncture, and the animals were killed by decapitation. The brain (cerebrum) was immediately removed from the cranium and frozen on dry ice. Blood samples were centrifuged, and plasma samples were stored at −80°C pending analysis for oxycodone and its metabolites.

For the brain analysis, the rat cerebrums were quickly thawed, weighed, and homogenized by a hand-held homogenizer (Tissue-Tearor; BioSpec Products, Bartlesville, Okla) in 10 volumes of 100-mmol/L borate buffer (pH 8.9). Internal standard was added, and the homogenate was centrifuged in a microcentrifuge at 8500*g* for 5 minutes. The pooled supernatant was subject to solid-phase extraction as described earlier for plasma and urine samples. Recovery of oxycodone and its metabolites from blank rat brain homogenates spiked with oxycodone and its metabolites was similar to that from plasma.

RESULTS

Human opioid receptor binding affinity of oxycodone and its metabolites. Table I presents a comparison of the affinity of oxycodone and its metabolites at the human μ-, human κ-, and mouse δ-opioid receptor as measured by their K_i values for competitive displacement of [^{3}H]-diprenorphine, a nonselective opioid antagonist. The data clearly demonstrate the μ-receptor selectivity of oxycodone and all of its metabolites as indicated by their nanomolar K_i values for the μ-receptor compared with micromolar K_i values for the κ- and δ-opioid receptors. For example, the affinity of noroxymorphone and oxymorphone toward κ- and δ-receptors was more than 15-fold lower than that at the μ-opioid receptor and is consistent with previously reported data.[9,41] This experiment further confirmed a previous comparison of μ-opioid receptor affinity between oxycodone and its primary *N*- and *O*-demethylated metabolites; that is, the affinity of oxycodone was 4-fold higher than that of noroxycodone and 40-fold lower than that of oxymorphone.[16] [^{3}H]-Diprenorphine displacement by noroxymorphone exhibited a K_i of 5.7 ± 1.2 nmol/L, which is intermediate between the parent drug and oxymorphone. The reduced metabolites of oxycodone (α- and β-oxycodol)

Table II. Mean estimates of noncompartmental pharmacokinetic parameters for oxycodone in 4 pilot study subjects, each receiving 10, 15, and 20 mg oral oxycodone

Oxycodone dose (mg)	*CL/F (L/min)*	*V_z/F (L)*	*t_{max} (min)*	*C_{max} (ng/mL)*	*$t_{½,z}$ (min)*	*$AUC_{0-\infty}$ (μg · min/mL)*
10	1.36 ± 0.23	413 ± 31.7	68 ± 8.7	25 ± 3	214 ± 25	7.5 ± 1.3
15	1.31 ± 0.21	465 ± 153	84 ± 33	36 ± 6	241 ± 45	11.6 ± 1.8
20	1.33 ± 0.48	454 ± 192	51 ± 21	43 ± 12	233 ± 23	16.4 ± 5.4

CL/F, Apparent clearance; V_z/F, apparent volume of distribution; t_{max}, time to maximum concentration; C_{max}, maximum concentration; $t_{½,z}$, terminal elimination half-life; $AUC_{0-\infty}$, area under plasma concentration–time curve extrapolated to infinity.

had lower but differing μ-receptor affinities compared with oxycodone; their K_i values were 2- and 12-fold higher than that of oxycodone, respectively. Morphine and DAMGO were included as references, with respective K_i values of 3.19 ± 0.43 nmol/L and 0.21 ± 0.03 nmol/L, which agree with reported values in the literature.[23,42]

μ-Opioid receptor–G-protein activation. Activation of the μ-opioid receptor by oxycodone and its metabolites, morphine, and DAMGO was measured by [^{35}S]-GTPγS binding to G_α proteins. The maximum activation (E_{max}) of morphine and oxycodone and its metabolites varied from 50% to 83% of that of DAMGO, indicating partial μ-opioid receptor activation. Oxycodone and its metabolites exhibited the same rank order of potency for the activation of [^{35}S]-GTPγS binding to CHO cell membrane expressing human μ-opioid receptor (EC_{50}) as the receptor binding affinity constant (K_i). Again, noroxymorphone exhibited intermediate activation potency between oxycodone and oxymorphone. Interestingly, the reduced products of oxymorphone, α- and β-oxymorphol, were nearly as potent as oxymorphone in the receptor activation assay. The most potent compounds in this series, oxymorphone and DAMGO, showed the highest maximum activation. EC_{50} and E_{max} for DAMGO and morphine (Table I) are consistent with values previously reported by Xu et al[43]: 59.4 ± 11.4 nmol/L and 247% ± 7%, respectively, for DAMGO and 56.4 ± 8.9 nmol/L and 201% ± 7%, respectively, for morphine.

Pharmacokinetics of plasma oxycodone and its metabolites. The main objective of our pharmacokinetic study was to characterize the plasma concentration–time course of oxycodone and its active metabolites after a single oral dose of the opioid. Particular attention was directed toward the products arising from the *N*-demethylation pathway (noroxycodone, α- and β-noroxycodol, and noroxymorphone) and the primary reduction of oxycodone (α- and β-oxycodol), which constitute the major active, non-CYP2D6 metabolites that have not been examined for their potential contribution to the pharmacodynamics of oxycodone. The pharmacokinetic analysis also included the plasma concentration–time course of the minor reductive metabolites of oxymorphone (α- and β-oxymorphol).

Table II presents the results of noncompartmental analysis of the plasma concentration–time data from the pilot study (ie, data from 4 subjects at the 3 dose levels). Oxycodone pharmacokinetics appeared to be dose-independent, as demonstrated by consistent estimates of V_z/F and CL/F across 3 doses in the 4 subjects.

The mean plasma concentration–time profiles of oxycodone and its metabolites after a 15-mg oral dose of oxycodone in all 16 subjects from both the pilot and main studies are shown in Fig 2. Table III presents a summary of the pharmacokinetic parameter estimates. The CL/F of oral oxycodone varied over a 2-fold range (1.1-2.0 L/min, or 12.8-25.9 mL · min^{-1} · kg^{-1}), and the V_z/F varied over a 2.5-fold range (270-690 L, or 4.0-9.3 L/kg). A somewhat higher mean CL/F per kilogram of body weight was noted for women compared with men (21.7 ± 3.2 mL · min^{-1} · kg^{-1} versus 17.9 ± 3.7 mL · min^{-1} · kg^{-1}), which was barely statistically significant ($P = .047$). No gender difference was noted for V_z/F: 5.9 ± 1.4 for women versus 5.8 ± 1.6 L/kg for men. The mean $t_{½,z}$ was 3.5 ± 0.8 hours.

The mean $t_{½,z}$ of the metabolites ranged from 4.6 hours for α-oxymorphol to as long as 11.6 hours for β-noroxycodol, with all values being longer than the $t_{½,z}$ for oxycodone (Fig 2). The plasma concentration of the *N*-demethylated metabolite noroxycodone was comparable to or exceeded the parent drug concentration in some individuals; the mean AUC_m/AUC_p was 1.2 ± 0.4. The *O*-demethylated metabolite oxymorphone had the lowest concentration of all circulating metabolites, with a mean C_{max} of only about 1 ng/mL and a low AUC_m/AUC_p of 0.04 ± 0.03. Plasma concentrations of oxymorphone were undetectable at late time points in several individuals. The didemethylated metabolite noroxymorphone was the

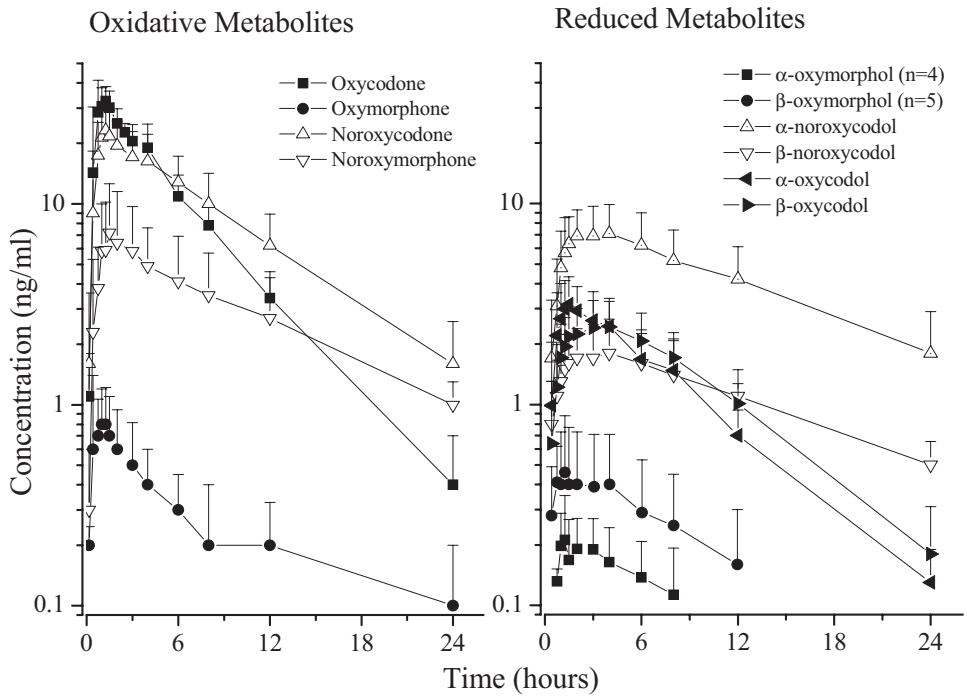

Fig 2. Mean plasma concentration–time course of oxycodone and its primary and secondary oxidative and reductive metabolites in 16 healthy human volunteers after single 15-mg oral dose of oxycodone.

Table III. Estimates of noncompartmental pharmacokinetic parameters for oxycodone and its primary and secondary oxidative and reductive metabolites in all 16 subjects receiving 15 mg oxycodone from both pilot and main studies

	CL/F (L/min)	*V_z/F (L)*	*t_{max} (h)*	*C_{max} (ng/mL)*	*$t_{½,z}$ (h)*	*AUC (μg · min/mL)*	*AUC_m/AUC_p*
Oxycodone	1.44 ± 0.31	431 ± 110	1.08 ± 0.45	38 ± 7.4	3.50 ± 0.83	10.8 ± 2.09	
Noroxycodone	—	—	1.22 ± 0.82	26 ± 8.2	5.82 ± 1.23	12.7 ± 4.77	1.19 ± 0.44
Oxymorphone	—	—	0.98 ± 0.47	1.1 ± 0.6	8.78 ± 4.35	0.41 ± 0.27	0.04 ± 0.03
Noroxymorphone	—	—	1.55 ± 0.78	7.8 ± 5.2	9.07 ± 2.23	5.07 ± 2.54	0.52 ± 0.35
α-Noroxycodol	—	—	2.72 ± 1.03	7.6 ± 2.6	10.05 ± 3.52	7.96 ± 3.82	0.66 ± 0.31
β-Noroxycodol	—	—	3.32 ± 1.75	1.9 ± 0.8	11.63 ± 4.98	1.93 ± 0.71	0.16 ± 0.06
α-Oxymorphol (n = 4)	—	—	1.56 ± 0.32	0.3 ± 0.1	5.38 ± 2.58	0.13 ± 0.08	0.01 ± 0.01
β-Oxymorphol (n = 5)	—	—	1.56 ± 0.59	0.4 ± 0.2	5.72 ± 5.43	0.21 ± 0.18	0.03 ± 0.04
α-Oxycodol	—	—	1.55 ± 0.57	3.5 ± 1.1	4.67 ± 1.31	1.62 ± 0.52	0.13 ± 0.04
β-Oxycodol	—	—	3.03 ± 1.20	2.6 ± 0.9	5.55 ± 1.66	1.83 ± 0.53	0.15 ± 0.04

Plasma concentrations of α- and β-oxymorphol were only detected in some of the subjects; the number of subjects is indicated in parentheses.
$AUC_{0-\infty}$, Area under plasma concentration–time curve; AUC_m/AUC_p, metabolite–to–parent drug area under plasma concentration–time curve ratio.

second most abundant species in circulation. This metabolite exhibited very high interindividual variability, as reflected in a C_{max} range of 0.03 to 1.55 ng/mL (mean, 7.8 ng/mL) and an AUC_m/AUC_p range of 0.7 to 21.5 (mean, 0.52). It had a relatively long $t_{½,z}$ of 9.1 ± 2.2 hours. The 1 subject with an exceptionally low noroxymorphone AUC also had the lowest oxymorphone AUC; this individual may be a CYP2D6 poor metabolizer, because we had previously shown that noroxymorphone is mainly derived from *O*-demethylation of noroxycodone by CYP2D6.[15,44]

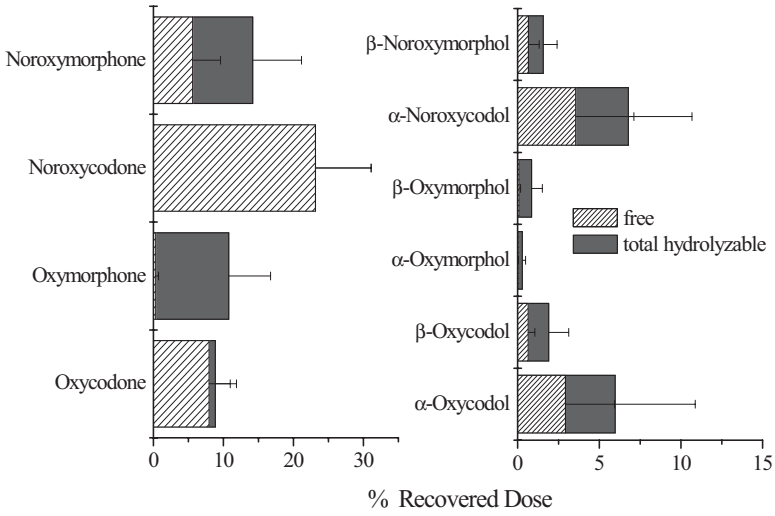

Fig 3. Mean 48-hour cumulative urinary recovery of oxycodone and its oxidative and reductive metabolites in 16 healthy subjects. *Hatched bars* representing the free, unconjugated fraction are overlaid with *gray bars* representing the total (hydrolyzable) fraction. The mean total recovery of oxycodone and its metabolites for the 16 subjects was 72% ± 19%, ranging from 46% to 105%.

Circulating concentrations of reduced metabolites were intermediate to those of noroxymorphone and oxymorphone, with AUC_m/AUC_p values of 0.13 and 0.15 for α- and β-oxycodol, respectively (Table III). The plasma concentrations of α- and β-oxycodol were comparable; the C_{max} values ranged from 2 to 5 ng/mL, with a mean $t_{½,z}$ of about 5 hours. The plasma concentration of α-noroxycodol was the highest of all reduced metabolites, 5-fold higher than that of β-noroxycodol, and only slightly lower than those of noroxymorphone. The β-noroxycodol concentration was comparable to the concentrations of the primary reduced metabolites α- and β-oxycodol. The reduced metabolites of oxymorphone (α- and β-oxymorphol) were detectable (>0.5 ng/mL) in only one third of the subjects.

Urinary excretion of oxycodone metabolites. Cumulative urinary excretion of oxycodone and its metabolites was measured over a 48-hour period (Fig 3); most of the excretion occurred over a period of 36 hours. On average, the total amount (ie, free plus conjugates) of oxycodone and its metabolites recovered in the pooled 48-hour urine accounted for 72% ± 19% of the administered oxycodone dose.

Oxycodone does not appear to undergo a significant degree of conjugation (at the 14-hydroxyl position) before its excretion, given that the recovery of oxycodone in urine after enzymatic hydrolysis was very similar to that of free or unhydrolyzed oxycodone (8.9% ± 2.6% versus 8.0% ± 2.6%). Noroxycodone was the major metabolite excreted in urine and, like oxycodone, does not appear to undergo conjugation (22.1% ± 9.0% hydrolyzed recovery versus 23.1% ± 7.6% unhydrolyzed recovery). The 3-*O*-demethyl-metabolites were excreted predominantly as conjugates; total oxymorphone accounted for 10.7% ± 5.5% of the oxycodone dose, with only 0.33% ± 0.4% of the dose being excreted as free oxymorphone. Total noroxymorphone accounted for 14.2% ± 7.5% of the oxycodone dose, which was 3-fold higher than that of free noroxymorphone (5.6% ± 3.6%).

Reduced metabolites (ie, α- and β-oxycodol, α- and β-noroxycodol, and α- and β-oxymorphol) in total accounted for about 18% of the dose as compared with 47% for oxidative metabolites (ie, oxymorphone, noroxycodone, and noroxymorphone) in urine. The metabolites α- and β-oxycodol and their conjugates represented about 8% of the dose: 6.0% ± 4.9% as α-oxycodone and 1.9% ± 1.2% as β-oxycodol, with an α-to-β ratio of about 3. Noroxycodols and their conjugates accounted for 9% of the dose: 6.8% ± 3.9% as α-noroxycodone and 1.6% ± 0.9% as β-noroxycodol. The reduced metabolites of oxymorphone and its conjugates constituted only about 1% of the dose.

The recovery of all products arising from primary, CYP2D6-mediated *O*-demethylation of oxycodone, namely, oxymorphone and its reduced metabolites, was 11% of the dose. The total recovery of primary, CYP3A-mediated *N*-demethylation of oxycodone

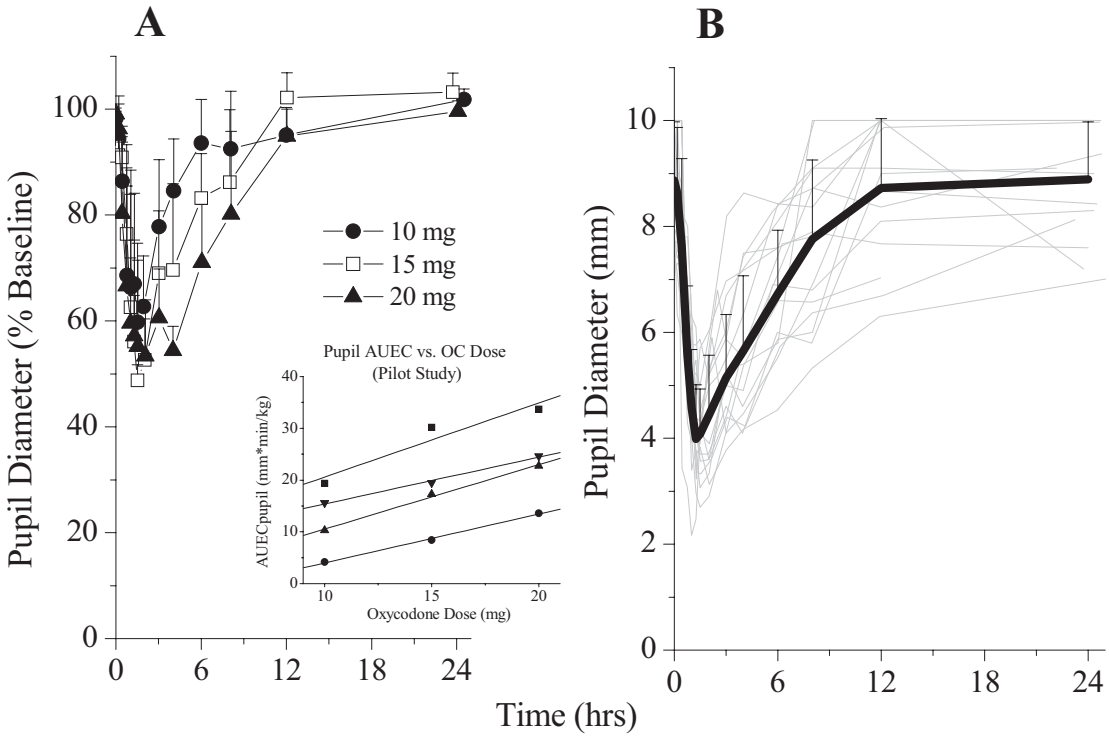

Fig 4. **A**, Time course of pupil diameter over 24-hour period in 4 subjects receiving 10-, 15-, and 20-mg oral does of oxycodone (pilot study). The *inset* depicts the linearity of the area under the effect curve (AUEC) for pupil response across the 3 doses in individual subjects. OC, Oxycodone. **B**, Individual time course of pupil diameter in 16 subjects after 15-mg dose of oxycodone (*gray lines*) in both pilot and main studies. The *black line* represents the mean pupil diameter over time. The mean AUEC from 0 to 24 hours was 1561 ± 628 mm · min, ranging from 311 to 2858 mm · min.

was 45% of the dose, which included 22% ± 9%, 9% ± 5%, and 14% ± 7% of the dose as noroxycodone, noroxycodone's reductive metabolites (α- and β-noroxycodol), and noroxymorphone, respectively.

Pupillometry and subjective side effects. The AUEC for pupil response to oxycodone was linearly related to dose for the 4 pilot subjects as displayed in Fig 4, *A*. Maximum pupil constriction did not exceed 60% of baseline (a decrease to 4 mm from a mean baseline value of 9 mm) at the highest dose (20 mg). Pupil diameter returned to the baseline value by 12 hours after dosing at all 3 dose levels. A composite plot of the individual time course of pupil constriction after the 15-mg oral dose of oxycodone in 12 main study subjects is presented in Fig 4, *B*. There was greater than 10-fold between-subject variability in AUEC for pupil response after the 15-mg oral dose of oxycodone. The AUEC for the decrease in pupil size ranged from 311 to 2858 mm · min, with a mean of 1561 ± 628 mm · min; there was 1 outlier with an AUEC that was 5-fold lower than the mean. A statistically significant (P = .046) smaller pupil AUEC was noted in men as compared with women; 2 men had the lowest AUEC values, and 3 of the highest AUEC values were seen in women.

Subjective ratings of side effects from the 15-mg oxycodone dose were generally mild, as demonstrated by the relatively low mean VAS ratings for nausea, pruritus, mood, and alertness scores over time as shown in Fig 5. Only 1 subject dropped out of the study because of unacceptable side effects. Maximum side effects occurred at similar times for all measures, 2 to 3 hours after dosing. The alertness score paralleled the pupil diameter change over time (Fig 4, *B*), although it is generally more variable across subjects.

Oxycodone PK-PD modeling. Plots of miotic effect versus plasma oxycodone concentration in the order of time revealed a counterclockwise hysteresis for all sub-

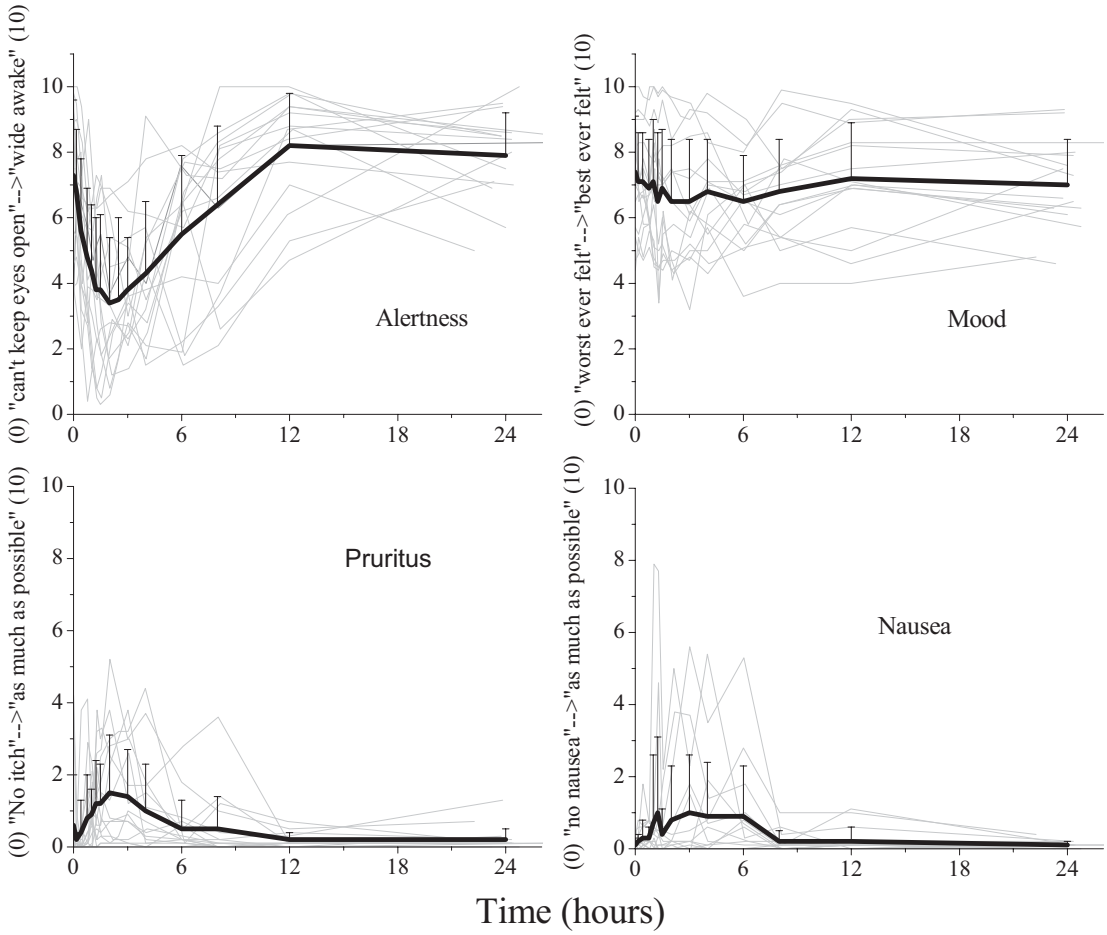

Fig 5. Visual analog scale ratings (10-cm scale) of subjective side effects over 24-hour period in healthy human volunteers (n = 16) who received 15-mg dose of oral oxycodone. Mean data (± SD) (*black lines*) are laid over individual profiles (*gray lines*).

jects in this study (Fig 6 shows examples in 4 representative subjects). The counterclockwise hysteresis can be explained by either a time lag in the distribution of oxycodone between the plasma and the central effect site or the contribution of active metabolite(s) that are formed and eliminated more slowly than the parent drug.

With respect to the active metabolite hypothesis, receptor binding and activation data have indicated that several of the oxycodone metabolites are sufficiently potent to warrant such consideration. To further explore and refine this hypothesis, we simulated the time course of receptor activation activity (expressed as percent increase in GTPγS binding) equivalent to the concentration of oxycodone versus each of the 3 major metabolites (ie, noroxycodone, noroxymorphone, and oxymorphone) present in circulation as predicted by the E_{max} model based on the E_{max} and EC_{50} data presented in Table I. The simulation of plasma receptor activity over time, as shown in Fig 7, suggested that oxycodone, along with noroxymorphone, appears to account for most of the available opioid receptor activity in circulation, particularly during the 6 to 8 hours after oxycodone administration. If it is assumed that the uptake of oxycodone metabolites into the central effect site(s) is comparable (see later), noroxymorphone was considered to be the most likely active metabolite to contribute to central opioid actions of oxycodone and was the metabolite of choice in the joint parent drug–metabolite PK-PD model. We compared fit of the miosis data with either a PK-PD model featuring delayed effect-site equilibration of oxycodone (ie, parent drug equilibration model) or a

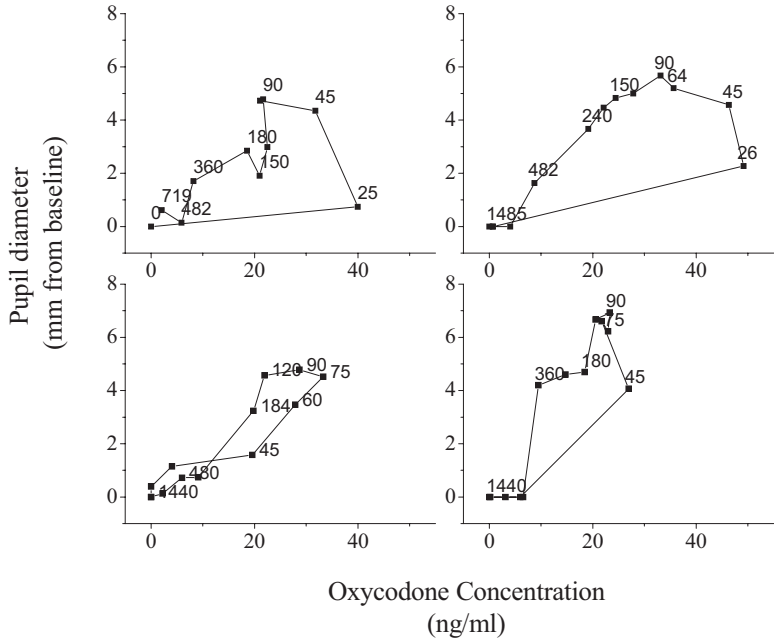

Fig 6. Representative constriction in pupil diameter versus plasma oxycodone concentration plots in 4 subjects. The number next to each data point indicates the elapsed time in minutes after oxycodone dosing. Counterclockwise hysteresis was evident in all subjects.

PK-PD model featuring the joint action of parent drug and noroxymorphone (active metabolite model) with or without an equilibration delay.

Data fit to the parent drug equilibration model converged in all cases with acceptable precision of model parameters. Both the KE0 program and the semiparametric PK-PD model implemented in SAAM II yielded nearly identical estimates of ke0. In contrast, for models that account for the joint effects of oxycodone and of noroxymorphone, either the fits failed to converge or, when there was convergence, the resultant parameter estimates had large confidence intervals that included 0 or the residual plots showed systematic deviation of the model predictions from the observed data (or both). Failure to converge or poor model fit was observed with individual subject data both from the main study at the dose level of 15 mg and from the individual data sets from the pilot study at multiple dose levels. In addition, we investigated the potential confounding resulting from "noisy" data when a numeric forcing function involving data interpolation was used. To examine the sensitivity of our joint parent drug–metabolite PK-PD model to the noise in plasma metabolite concentration data, "data smoothing" was accomplished by use of a multiexponential fit of the metabolite data or exclusion of outlying, noisy data

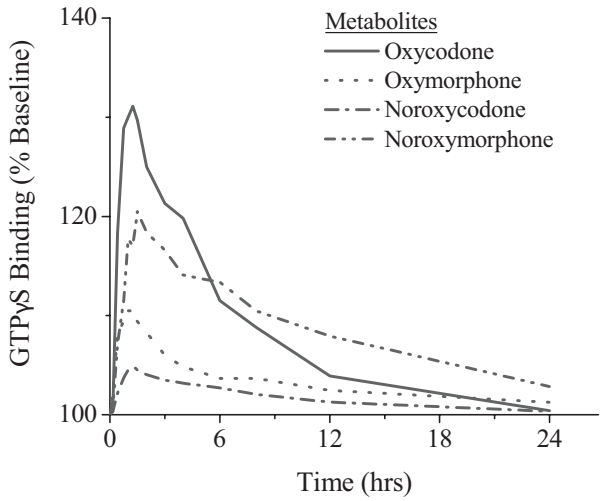

Fig 7. Simulation of time course of plasma μ-opioid receptor activation activity equivalent to circulating concentration of oxycodone and its 3 oxidative metabolites according to maximum activation (E_{max}) model and by use of guanosine-5′-*O*-(γ-thio[triphosphate]) (GTPγS) binding parameters presented in Table I.

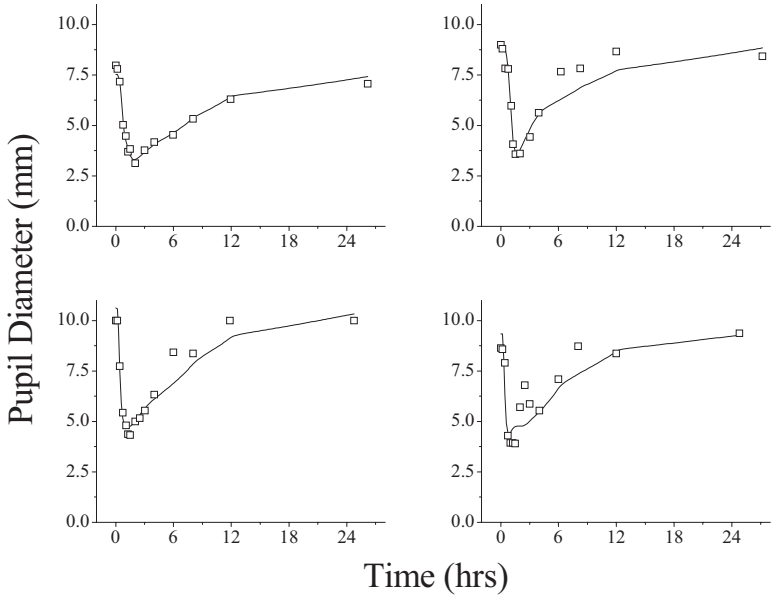

Fig 8. Oxycodone pharmacokinetic-pharmacodynamic model prediction of pupil diameter (*lines*) and observed data (*squares*) illustrated in 4 representative subjects receiving 15 mg oxycodone.

Table IV. Pharmacodynamic model parameter estimates (equation 1) for time course of pupil constriction after 15 mg oral oxycodone in healthy human volunteers

	EC_{50}	E_0	*ke0*	$t_{½,e0}$
Mean	30 ng/mL	9.2 mm	0.1 1/min	11 min
SD	15 ng/mL	1.3 mm	0.09 1/min	6 min
Coefficient of variation	50%	13.8%	95.1%	55%
Range	12-71 ng/mL	7.5-10.9 mm	0.03-0.4 1/min	2-26 min

E_0, Baseline pupil diameter; ke0, effect site equilibration rate constant; $t_{½,e0}$, effect site equilibration half life.

points. These approaches failed to result in any improvements in fit for the parent drug–metabolite PK-PD model. Hence we conclude that the likely explanation for the counterclockwise hysteresis plot is an equilibration delay of the oxycodone effect.

Examples of the goodness of fit with the parent drug equilibration model to the observed data are shown in Fig 8. The classical E_{max} model was used to fit the effector site concentration to the observed response. We did assess the need for a more general sigmoid E_{max} model. When the Hill coefficient γ was allowed to vary, the parameter estimate ranged from 0.9 to 2.8. In 18 of 24 data sets, the 95% confidence intervals for γ included unity. Hence, we adopted a parsimonious approach by fixing γ at a value of 1 (ie, in effect, a classical E_{max} model). Parameter estimates derived from the final nonlinear regression analysis of the 15-mg dose data are presented in Table IV. In a follow-up exercise parameter estimates obtained from a simultaneous fit of the model to the multidose data from the pilot study were not significantly different from the estimates obtained with the 15-mg dose data for all 16 subjects.

A variation in the effect site equilibration half life ($t_{½,e0}$) of more than 10-fold was observed, from 2 to 26 minutes. The individual EC_{50} values were well estimated, except for 3 of 16 individuals. In those 3 subjects the ke0 estimate reached very high values ($t_{½,e0}$ $<$5 minutes) with coefficients of variation of greater than 80%, indicating a lack of a clearly discernible equilibration delay. In these individuals estimates of EC_{50} did not differ appreciably between the case when ke0 was left to float and when ke0 was fixed to a value of 10 min^{-1}, corresponding to a $t_{½,e0}$ of about 4 seconds. Whereas EC_{50} estimates ranged from 12 to 71 ng/mL for the entire set of subjects, the 2 individuals

Table V. Brain and plasma concentrations and brain-to-plasma distribution ratios of oxycodone and its metabolites in Wistar rats (N = 5) after intragastric administration of 10 mg/kg oxycodone

	Oxycodone	*Noroxycodone*	*Oxymorphone*	*Noroxymorphone*	β-*Oxycodol*
Plasma concentration (ng/mL)	107 ± 48	814 ± 109	66.6 ± 10.3	695 ± 158	38.8 ± 13.4
Brain concentration (ng/g)	215 ± 46	91.8 ± 39.6	15.6 ± 4.5	5.9 ± 1.5	10.5 ± 4.5
Brain/plasma ratio	2.07 ± 0.62	0.10 ± 0.04	0.23 ± 0.09	0.008 ± 0.003	0.25 ± 0.09
Brain AUC_m/AUC_p (%)	100	5.9	0.48	0.18	2.25
LogD* (pH 7-8)	1.2 to 1.7	−0.4 to 0.45	0.5 to 0.9	−1.15 to 0.29	0.7 to 1.16
LogP*	1.8 ± 0.6	1.1 ± 0.6	1.1 ± 0.6	0.3 ± 0.6	1.26 ± 0.6

On the basis of the assumption that there were similar distribution ratios in rats and humans, the relative abundance of metabolites in the brain was predicted by multiplying plasma AUC_m/AUC_p in Table III by the metabolite-to-drug ratio in brain-to-plasma partitioning.

LogD, Computed or experimental octanol/buffer partitioning coefficients calculated at pH 7 and pH 8; LogP, computed octanol/water partitioning coefficients.

*Estimates from SciFinder (CAS, American Chemical Society, Columbus, Ohio) by use of ACD Solaris Software V4.67. There was reasonable agreement with measured logD values (at pH 7.4) of 1.65 for oxycodone and 0.99 for oxymorphone reported by Plummer et al.[59]

with exceptionally high EC_{50} values of 58 and 71 ng/mL also had high ke0 values. Exclusion of the outliers resulted in a slight decrease in mean EC_{50} but a sizable decrease in the interindividual coefficient of variation, from 50% to 30%. The marginally statistically significant gender difference observed in oxycodone clearance did not translate into statistically significant differences in oxycodone pharmacodynamic parameters with respect to gender or body weight.

Brain distribution of oxycodone and its metabolites in rats. To provide additional information on the significance of oxycodone metabolites, or the lack thereof, in the pharmacodynamics of oxycodone, brain-to-plasma distribution ratios of oxycodone and its metabolites were determined at 60 minutes after a 10-mg/kg intragastric dose of oxycodone in a group of rats (n = 5). The data presented in Table V clearly show that oxycodone was concentrated in the rat cerebrum, with a brain-to-plasma ratio of approximately 2. In contrast, the brain-to-plasma concentration ratios of all 3 oxidative metabolites were well under unity (<0.01 to 0.25). The noroxymorphone concentration in the brain was particularly low, at less than 1% of the plasma concentrations. Table V also includes the predicted abundance of oxycodone metabolites in the human brain as a percentage of oxycodone based on their relative abundance in plasma, with the assumption that the metabolites have the same brain distribution ratios in humans as in rats. The predictions argue for a very low presence of oxycodone metabolites in the brain relative to the parent drug (ie, at <6%).

DISCUSSION

This study offers new insights into the metabolism, pharmacokinetics, and pharmacodynamics of oxycodone. With respect to the metabolism and pharmacokinetics of oxycodone, our study provides the first quantitative accounting of oxycodone metabolism in humans and extends the available information on the pharmacokinetics of oxycodone metabolites in circulation.

The pharmacokinetic parameters of oral oxycodone reported in Tables II and III agree with results from earlier studies in healthy human volunteers.[4,45] The reported clearance of intravenous oxycodone is reasonably high (approximately 0.8 L/min), which predicts a medium hepatic extraction and a moderate first-pass effect.[46,47] In fact, the systemic availability of orally administered oxycodone has been determined to be between 60% and 80%. All of these data explain our observation of a relatively high mean oral clearance of oxycodone, at 1.4 L/min. The circulating concentrations of noroxycodone and oxymorphone observed in this study are also consistent with previous reports.[13,14] Plasma concentrations of noroxycodone were slightly higher than or comparable to those of oxycodone, whereas plasma oxymorphone concentrations were much lower than those of oxycodone and barely measurable in some subjects. We also observed significant circulating concentrations of noroxymorphone and the reduced metabolites of oxycodone (α- and β-oxycodol) and noroxycodone (α- and β-noroxycodol), which are new findings. The mean plasma metabolite–to–parent drug AUC ratio for noroxymorphone was 0.52 ± 0.35. A slightly higher AUC ratio was also observed for the combined presence of α- and β-noroxycodol, with α-noroxycodol being the predominant epimer in circulation. The concentrations of these secondary metabolites of oxycodone *N*-demethylation were only slightly lower than those of their precursor, noroxycodone. The reduced metabolites of oxycodone were present at lower concentrations (about one third those of noroxycodols) and did not show any stereoselectivity in formation. Reduced metabolites of oxymorphone were

also detected, but their concentrations were less than a tenth of those of the other reduced metabolites and no higher than those of oxymorphone.

The oxycodone metabolite profile in urine is consistent with findings from our earlier in vitro metabolic studies with oxycodone in human liver microsomes.[15] In vitro, microsomal oxidation via CYP3A-mediated *N*-demethylation was the predominant pathway. Intrinsic clearance (ie, maximum velocity/Michaelis-Menten constant) for CYP3A-mediated *N*-demethylation of oxycodone was, on average, 7-fold higher than CYP2D6-mediated *O*-demethylation. The same is true in vivo. The 48-hour urinary recovery of products from the *N*-demethylation pathway (noroxycodone, α- and β-noroxycodol, and noroxymorphone) was, on average, 4.8 ± 2.6–fold greater than that of products from the *O*-demethylation pathway (oxymorphone and α- and β-oxymorphol). Oxymorphone is excreted in urine largely in the form of conjugates (Fig 3). Cone et al[48] reported extensive conjugation of oxymorphone when it is administered as an oral solution to human subjects, and we have tentatively identified the major conjugate product to be oxymorphone-3-glucuronide in urine and plasma samples by LC-MS. Thus the very low plasma concentrations of oxymorphone could be the result of both its limited formation and its efficient elimination via 3-*O*-glucuronidation. The recovery of oxycodols in urine accounted for about 10% of the dose, most of which are presumed to be in the form of 6-*O*-conjugates; hence reduction is a minor pathway in the clearance of oxycodone. It should be noted that, on average, the currently identified metabolites in urine account for about 72% of the oral oxycodone dose. Whether the remainder of the dose (approximately 28%) represents either yet to be identified metabolic or excretory pathways (or both) or incomplete gastrointestinal absorption is not known. We were not able to confirm the recently reported presence of *N*-oxide metabolites of oxycodone in urine from individuals who abused oxycodone or had an overdose.[49]

The most important finding from our study concerns the putative role of circulating active metabolites in the pharmacodynamics of oxycodone. There has long been a debate as to the role of active metabolites in the pharmacologic actions of oxycodone. The antinociceptive potency of oxycodone in rodents is nearly equal to that of morphine.[8,39] Clinical studies also yielded similar observations; the median consumption of intravenous morphine was 80% that of intravenous oxycodone in patients with cancer receiving patient-controlled analgesia.[5] However, oxycodone is a weaker μ-opioid receptor agonist than morphine. Our current radioligand displacement study showed that the μ-receptor affinity of oxycodone is only one fifth that of morphine, whereas its potency in activating GTPγS binding to the μ-receptor is about one third that of morphine (Table I). This apparent discrepancy has been hypothesized to be the result of either the involvement of active metabolites[5] or the combined actions of oxycodone at the μ- and κ-opioid receptors, as suggested by recent animal studies.[50,51] The latter hypothesis is unlikely in view of our failure to show a significant affinity of oxycodone for the κ-receptor (K_i <1 μmol/L). There have been several attempts to identify active metabolite(s) of oxycodone that contribute to its opioid effects. As was mentioned previously, 3-*O*-demethylation of codeine to morphine by CYP2D6 is generally accepted as a major determinant of the analgesic efficacy of codeine.[6,7,12] Available data suggest that the same activation mechanism does not apply to the other closely related 3-*O*-methyl derivatives of 6-keto-opioids (dihydrocodeine, hydrocodone, and oxycodone), even though in each case *O*-demethylation results in the formation of a highly potent opioid agonist.[12,13,52–55] A recent study by Heiskanen et al[13] in healthy humans showed that the psychomotor and subjective side effects of oxycodone were unaffected by pretreatment with quinidine, a potent CYP2D6 inhibitor. Pharmacokinetic studies indicated that the circulating concentrations of the 3-*O*-demethyl-metabolite of oxycodone, oxymorphone, were barely detectable in control subjects, which explains the lack of effect from inhibition of CYP2D-mediated 6-*O*-demethylation of oxycodone. This led us to explore the possibility that other circulating active opioid metabolites may contribute to oxycodone pharmacodynamics.

The non-CYP2D6 metabolites of interest included the *N*-demethylation products (noroxycodone, noroxymorphone, and noroxycodols) and the reduction products of oxycodone (oxycodols). The potential for a metabolite to contribute to the in vivo opioid activity of oxycodone depends on its potency at the μ-receptor and relative abundance in circulation or, more appropriately, at the site of action. Even though noroxycodone is the most abundant metabolite in circulation, its potential to contribute to the opioid actions of oxycodone is not likely because of its relatively low potency in displacing radioligand and activating G protein at the expressed human μ-opioid receptor. Also, it has been reported that noroxycodone has a 3-fold higher half-maximal effective dose (ED_{50}) compared with oxycodone in a tail-flick antinociceptive assay after intracerebroventricular

administration in the rat.[17] In comparison, noroxymorphone, the didemethylated metabolite of oxycodone, exhibits receptor affinity and G-protein activation that is 3-fold higher than that of oxycodone and comparable to that of morphine. The formation of noroxymorphone proceeds by way of the catalytically efficient CYP2D6 *O*-demethylation of noroxycodone.[15] As a result, noroxymorphone is reasonably abundant in circulation (ie, about one half of the concentration of its 2 precursors, oxycodone and noroxycodone). The potential for noroxymorphone to contribute to the opioid activity of oxycodone was supported by the prediction of the time course of GTPγS binding activity based on the circulating concentration of the various active metabolites of oxycodone. The simulation suggests that noroxymorphone may be the putative metabolite that binds to the opioid receptors in addition to the parent drug in plasma samples from subjects administered oxycodone.[5] An additional contribution from the reduced metabolites is not very likely. β-Oxycodol demonstrated a 2-fold lower binding affinity for the μ-opioid receptor compared with oxycodone, as indicated by the [^{3}H]-diprenorphine displacement K_i value, whereas α-oxycodol had a 12-fold lower affinity. Likewise, α- and β-oxycodol displayed half-maximal receptor activation concentrations (EC_{50}) that were 6- and 20-fold lower, respectively, than those of oxycodone.

The result from our PK-PD modeling of the miotic response to oxycodone was initially surprising. There was no indication that the circulating active metabolites, in particular, noroxymorphone, contributed to oxycodone pharmacodynamics. The time course of the plasma oxycodone concentration adequately explained the time course of pupil constriction. Indeed, the duration of pupil constriction and subjective side effects, being 10 to 12 hours after dosing of oxycodone, is more in line with the plasma $t_{½}$ of oxycodone (3.5 hours) than that of the metabolites (5-11 hours). The lack of a metabolite contribution toward the pharmacodynamics of oxycodone is explained by the differential access of oxycodone and its metabolites to the central site of action. The tissue distribution study in the rat demonstrated remarkable differences in brain uptake between the major active circulating metabolites and oxycodone. The brain-to-plasma concentration ratios of oxycodone metabolites were much lower than those of the parent drug. The variation in brain uptake between oxycodone and its metabolites appears to correlate with their differences in lipophilicity, as indicated by the computed octanol-water partition coefficient (logD) of these compounds. The brain-to-plasma partition ratios of oxymorphone and noroxycodone are in the range of those of morphine, at 0.23 ± 0.03.[56] In contrast, the brain-to-plasma concentration ratio of oxycodone is nearly 10-fold higher; moreover, it is 2-fold higher than the reported steady-state brain-to-plasma AUC ratio of codeine in the rat (0.99 ± 0.25).[57] The large difference between blood-brain barrier penetration of oxycodone versus morphine offers an explanation for the apparent inconsistency between their in vitro potency at the μ-opioid receptor and antinociceptive or analgesic efficacy (ED_{50}) in vivo. Noroxymorphone, which held the most promise for contributing to the pharmacodynamics of oxycodone, has an extremely low brain-to-plasma partitioning, at lower than 1%, which is a consequence of its secondary amine structure compared with the tertiary amine structure of oxycodone. Thus *N*- and *O*-demethylation of oxycodone lead to metabolites with a markedly lower logD and consequently reduced permeability across the blood-brain barrier.[58]

In conclusion, we demonstrated that the time course of central opioid effects of oxycodone can be explained by the PK-PD of the parent drug alone. Although it was shown that the potent active metabolite noroxymorphone is present at relatively high concentrations in circulation, it does not appear to penetrate the blood-brain barrier to a significant extent. Other metabolites either demonstrate low potency (noroxycodone and β-noroxycodol) or are present in circulation at very low levels (oxymorphone and α- and β-oxycodol). In addition, all metabolites demonstrate restricted brain penetration as compared with the parent drug.

We thank Dr Peng Huang at Temple University for technical guidance with the opioid receptor activation assay, Ziping Yang at the University of Washington for culturing of CHO cells expressing opioid receptors, and Dr Paolo Vicini at the University of Washington Resource Facility for Population Kinetics for his assistance in PK-PD modeling.

Dr Shen received an honorarium from Purdue Pharma LP (Stamford, Conn) for consulting and conducting a seminar after the work described herein was completed. The other authors have no conflict of interest.

References

1. Davis MP, Varga J, Dickerson D, Walsh D, LeGrand SB, Lagman R. Normal-release and controlled-release oxycodone: pharmacokinetics, pharmacodynamics, and controversy. Support Care Cancer 2003;11:84-92.

2. Rischitelli DG, Karbowicz SH. Safety and efficacy of controlled-release oxycodone: a systematic literature review. Pharmacotherapy 2002;22:898-904.
3. Patt RB. Using controlled-release oxycodone for the management of chronic cancer and noncancer pain. American Pain Society Bulletin 1996;6:1-5.
4. Poyhia R, Vainio A, Kalso E. A review of oxycodone's clinical pharmacokinetics and pharmacodynamics. J Pain Symptom Manage 1993;8:63-7.
5. Kalso E, Vainio A, Mattila MJ, Rosenberg PH, Seppala T. Morphine and oxycodone in the management of cancer pain: plasma levels determined by chemical and radioreceptor assays. Pharmacol Toxicol 1990;67:322-8.
6. Caraco Y, Tateishi T, Guengerich FP, Wood AJ. Microsomal codeine N-demethylation: cosegregation with cytochrome P4503A4 activity. Drug Metab Dispos 1996; 24:761-4.
7. Poulsen L, Brosen K, Arendt-Nielsen L, Gram LF, Elbaek K, Sindrup SH. Codeine and morphine in extensive and poor metabolizers of sparteine: pharmacokinetics, analgesic effect and side effects. Eur J Clin Pharmacol 1996;51:289-95.
8. Duttaroy A, Yoburn BC. The effect of intrinsic efficacy on opioid tolerance. Anesthesiology 1995;82:1226-36.
9. Metzger TG, Paterlini MG, Ferguson DM, Portoghese PS. Investigation of the selectivity of oxymorphone- and naltrexone-derived ligands via site-directed mutagenesis of opioid receptors: exploring the "address" recognition locus. J Med Chem 2001;44:857-62.
10. Schidhammer H, Kaspar F, Marki A, Borsodi A. Mixed azines with dihydromorphinone derivatives. Helv Chim Acta 1994;77:999-1002.
11. Thompson CM, Wojno H, Greiner E, May EL, Rice KC, Selley DE. Activation of G-proteins by morphine and codeine congeners: insights to the relevance of O- and N-demethylated metabolites at mu- and delta-opioid receptors. J Pharmacol Exp Ther 2004;308:547-54.
12. Cleary J, Mikus G, Somogyi A, Bochner F. The influence of pharmacogenetics on opioid analgesia: studies with codeine and oxycodone in the Sprague-Dawley/Dark Agouti rat model. J Pharmacol Exp Ther 1994;271:1528-34.
13. Heiskanen T, Olkkola KT, Kalso E. Effects of blocking CYP2D6 on the pharmacokinetics and pharmacodynamics of oxycodone. Clin Pharmacol Ther 1998;64:603-11.
14. Kaiko RF, Benziger DP, Fitzmartin RD, Burke BE, Reder RF, Goldenheim PD. Pharmacokinetic-pharmacodynamic relationships of controlled-release oxycodone. Clin Pharmacol Ther 1996;59:52-61.
15. Lalovic B, Phillips B, Risler LL, Howald W, Shen DD. Quantitative contribution of CYP2D6 and CYP3A to oxycodone metabolism in human liver and intestinal microsomes. Drug Metab Dispos 2004;32:447-54.
16. Chen ZR, Irvine RJ, Somogyi AA, Bochner F. Mu receptor binding of some commonly used opioids and their metabolites. Life Sci 1991;48:2165-71.
17. Leow KP, Smith MT. The antinociceptive potencies of oxycodone, noroxycodone and morphine after intracerebroventricular administration to rats. Life Sci 1994;54: 1229-36.
18. Lalovic B, Wendel WL, Shen DD. Reductive metabolism of oxycodone in human liver microsomes and cytosol. In: Abstracts of the Tenth World Congress on Pain; 2002 Aug; San Diego, Calif. Seattle: IASP Press; 2002. p. 331.
19. Evans CJ, Keith DE Jr, Morrison H, Magendzo K, Edwards RH. Cloning of a delta opioid receptor by functional expression. Science 1992;258:1952-5.
20. Huang P, Kehner GB, Cowan A, Liu-Chen LY. Comparison of pharmacological activities of buprenorphine and norbuprenorphine: norbuprenorphine is a potent opioid agonist. J Pharmacol Exp Ther 2001;297:688-95.
21. Li S, Zhu J, Chen C, Chen YW, Deriel JK, Ashby B, et al. Molecular cloning and expression of a rat kappa opioid receptor. Biochem J 1993;295(Pt 3):629-33.
22. Zhu J, Luo LY, Li JG, Chen C, Liu-Chen LY. Activation of the cloned human kappa opioid receptor by agonists enhances [35S]GTPgammaS binding to membranes: determination of potencies and efficacies of ligands. J Pharmacol Exp Ther 1997;282:676-84.
23. Gillen C, Haurand M, Kobelt DJ, Wnendt S. Affinity, potency and efficacy of tramadol and its metabolites at the cloned human mu-opioid receptor. Naunyn Schmiedebergs Arch Pharmacol 2000;362:116-21.
24. Gabrielsson J, Weiner D. PK/PD data analysis: concepts and applications. 2nd ed. Stockholm: Swedish Pharmaceutical Press; 1998. p. 450-67.
25. Bitsios P, Szabadi E, Bradshaw CM. Comparison of the effects of venlafaxine, paroxetine and desipramine on the pupillary light reflex in man. Psychopharmacology (Berl) 1999;143:286-92.
26. Phillips MA, Bitsios P, Szabadi E, Bradshaw CM. Comparison of the antidepressants reboxetine, fluvoxamine and amitriptyline upon spontaneous pupillary fluctuations in healthy human volunteers. Psychopharmacology (Berl) 2000;149:72-6.
27. Schmitt JA, Riedel WJ, Vuurman EF, Kruizinga M, Ramaekers JG. Modulation of the critical flicker fusion effects of serotonin reuptake inhibitors by concomitant pupillary changes. Psychopharmacology (Berl) 2002; 160:381-6.
28. Phimmasone S, Kharasch ED. A pilot evaluation of alfentanil-induced miosis as a noninvasive probe for hepatic cytochrome P450 3A4 (CYP3A4) activity in humans. Clin Pharmacol Ther 2001;70:505-17.
29. Coda BA, Brown MC, Risler L, Syrjala K, Shen DD. Equivalent analgesia and side effects during epidural and pharmacokinetically tailored intravenous infusion with matching plasma alfentanil concentration. Anesthesiology 1999;90:98-108.
30. Erjavec MK, Coda BA, Nguyen Q, Donaldson G, Risler L, Shen DD. Morphine-fluoxetine interactions in healthy

volunteers: analgesia and side effects. J Clin Pharmacol 2000;40:1286-95.
31. Romberg RW, Lee L. Comparison of the hydrolysis rates of morphine-3-glucuronide and morphine-6-glucuronide with acid and beta-glucuronidase. J Anal Toxicol 1995; 19:157-62.
32. Barrett PH, Bell BM, Cobelli C, Golde H, Schumitzky A, Vicini P, et al. SAAM II: Simulation, Analysis, and Modeling Software for tracer and pharmacokinetic studies. Metabolism 1998;47:484-92.
33. Kowalski KG, Karim A. A semicompartmental modeling approach for pharmacodynamic data assessment. J Pharmacokinet Biopharm 1995;23:307-22.
34. Mager DE, Wyska E, Jusko WJ. Diversity of mechanism-based pharmacodynamic models. Drug Metab Dispos 2003;31:510-8.
35. Sheiner LB, Stanski DR, Vozeh S, Miller RD, Ham J. Simultaneous modeling of pharmacokinetics and pharmacodynamics: application to d-tubocurarine. Clin Pharmacol Ther 1979;25:358-71.
36. DiPalma JR. Drill's pharmacology in medicine. New York: McGraw Hill; 1965. p. 90.
37. Shafer S. KE0 Program. Stanford PK/PD software server. Available from: URL:http://anesthesia.stanford.edu/pkpd/Other%20Utilities/. Accessed March 14, 2006.
38. Unadkat JD, Bartha F, Sheiner LB. Simultaneous modeling of pharmacokinetics and pharmacodynamics with nonparametric kinetic and dynamic models. Clin Pharmacol Ther 1986;40:86-93.
39. Poyhia R, Kalso EA. Antinociceptive effects and central nervous system depression caused by oxycodone and morphine in rats. Pharmacol Toxicol 1992;70:125-30.
40. Ross FB, Wallis SC, Smith MT. Co-administration of sub-antinociceptive doses of oxycodone and morphine produces marked antinociceptive synergy with reduced CNS side-effects in rats. Pain 2000;84:421-8.
41. Yoburn BC, Shah S, Chan K, Duttaroy A, Davis T. Supersensitivity to opioid analgesics following chronic opioid antagonist treatment: relationship to receptor selectivity. Pharmacol Biochem Behav 1995;51:535-9.
42. Raynor K, Kong H, Mestek A, Bye LS, Tian M, Liu J, et al. Characterization of the cloned human mu opioid receptor. J Pharmacol Exp Ther 1995;272:423-8.
43. Xu H, Lu YF, Rothman RB. Opioid peptide receptor studies. 16. Chronic morphine alters G-protein function in cells expressing the cloned mu opioid receptor. Synapse 2003;47:1-9.
44. Cascorbi I. Pharmacogenetics of cytochrome p4502D6: genetic background and clinical implication. Eur J Clin Invest 2003;33(Suppl 2):17-22.
45. Poyhia R, Seppala T, Olkkola KT, Kalso E. The pharmacokinetics and metabolism of oxycodone after intramuscular and oral administration to healthy subjects. Br J Clin Pharmacol 1992;33:617-21.
46. Leow KP, Smith MT, Williams B, Cramond T. Single-dose and steady-state pharmacokinetics and pharmacodynamics of oxycodone in patients with cancer. Clin Pharmacol Ther 1992;52:487-95.
47. Poyhia R, Olkkola KT, Seppala T, Kalso E. The pharmacokinetics of oxycodone after intravenous injection in adults. Br J Clin Pharmacol 1991;32:516-8.
48. Cone EJ, Darwin WD, Buchwald WF, Gorodetzky CW. Oxymorphone metabolism and urinary excretion in human, rat, guinea pig, rabbit, and dog. Drug Metab Dispos 1983;11:446-50.
49. Moore KA, Ramcharitar V, Levine B, Fowler D. Tentative identification of novel oxycodone metabolites in human urine. J Anal Toxicol 2003;27:346-52.
50. Nielsen CK, Ross FB, Smith MT. Incomplete, asymmetric, and route-dependent cross-tolerance between oxycodone and morphine in the Dark Agouti rat. J Pharmacol Exp Ther 2000;295:91-9.
51. Ross FB, Smith MT. The intrinsic antinociceptive effects of oxycodone appear to be kappa-opioid receptor mediated. Pain 1997;73:151-7.
52. Kaplan HL, Busto UE, Baylon GJ, Cheung SW, Otton SV, Somer G, et al. Inhibition of cytochrome P450 2D6 metabolism of hydrocodone to hydromorphone does not importantly affect abuse liability. J Pharmacol Exp Ther 1997;281:103-8.
53. Lelas S, Wegert S, Otton SV, Sellers EM, France CP. Inhibitors of cytochrome P450 differentially modify discriminative-stimulus and antinociceptive effects of hydrocodone and hydromorphone in rhesus monkeys. Drug Alcohol Depend 1999;54:239-49.
54. Schmidt H, Vormfelde SV, Walchner-Bonjean M, Klinder K, Freudenthaler S, Gleiter CH, et al. The role of active metabolites in dihydrocodeine effects. Int J Clin Pharmacol Ther 2003;41:95-106.
55. Webb JA, Rostami-Hodjegan A, Abdul-Manap R, Hofmann U, Mikus G, Kamali F. Contribution of dihydrocodeine and dihydromorphine to analgesia following dihydrocodeine administration in man: a PK-PD modelling analysis. Br J Clin Pharmacol 2001;52:35-43.
56. Murphey LJ, Olsen GD. Diffusion of morphine-6-beta-D-glucuronide into the neonatal guinea pig brain during drug-induced respiratory depression. J Pharmacol Exp Ther 1994;271:118-24.
57. Xie R, Hammarlund-Udenaes M. Blood-brain barrier equilibration of codeine in rats studied with microdialysis. Pharm Res 1998;15:570-5.
58. Clark DE. In silico prediction of blood-brain barrier permeation. Drug Discov Today 2003;8:927-33.
59. Plummer JL, Cmielewski PL, Reynolds GD, Gourlay GK, Cherry DA. Influence of polarity on dose-response relationships of intrathecal opioids in rats. Pain 1990;40: 339-47.